Proceedings of the International MultiConference of Engineers and Computer Scientists 2015 Vol II,
IMECS 2015, March 18 - 20, 2015, Hong Kong

Enhanced Mathematical Model for Studying Fundamental Behaviors of Injection Locked Relaxation Oscillator

A. Kitipongwatana, P. Koseeyaporn, J. Koseeyaporn, and P. Wardkein

***Abstract*—This article proposes the analytical model for studying behaviors of injection locked relaxation oscillator (ILRO). The proposed model enhanced from N. Soltani's model can be used to demonstrate behaviors of the ILRO in case the input frequency is higher than the natural frequency, namely, necessarily physical conditions for locking, locked ranges, detuning behaviors and frequency division. The proposed model is verified by simulation results of the ILRO based on 0.35um-CMOS technology of TSMC.**

***Index Terms*— Injection locked relaxation oscillator (ILRO), Locking condition, Locked range, Detuning.**

I. Introduction

BASED on interesting behaviors of an injection locked oscillator, many mathematical models were proposed which are divided into 2 main groups, namely, the manual analytical models and the analytical models using numerical methods to determine the solutions. With the pattern of analysis of the first group [1-3], profound understanding to the influence of the parameters appearing in the system on the detuning and locking processes is possible. However, these models are limited to the harmonic oscillator. For the other group [4-6], the method can be employed to determine the accurate solutions of both the harmonic and non-harmonic oscillators which are fed by an input signal but it is not yet a suitable tool for deeply understand the detuning and locking process.

In 2010, the manual analytical model for ILRO was proposed by N. Sotani et al. [7]. But only the input frequency around the natural frequency was considered and the explanation of the detuning process is quite difficult to relate with the practical results. However, in this paper, the model in [7] is enhanced in order to explain the detuning and locking processes when the input frequency is higher than the natural frequency.

An organization of this article begins with the fundamental relaxation oscillator in section 2. Studying behaviors of ILRO is discussed in section 3. Section 4 is to demonstrate comparisons between simulation results and calculation results. Finally, section 5 is for conclusion of this article.

Manuscript received December 04, 2014; revised January 08, 2015. Financial support from the Thailand Research Fund through the Royal Golden Jubilee Ph.D. Program (Grant No. PHD/0014/2553) to Arum Kitipongwatana and Paramote Wardkein are acknowledged.

A. Kitipongwatana is with Faculty of Engineering, King Mongkut's Institute of Technology Ladkrabang, Ladkrabang, Bangkok, 10520, THAILAND (e-mail: Akami000@gmail.com).

P. Koseeyoporn is with Faculty of Technical Education, Department of Teacher Training in Electrical Engineering, King Mongkut's University of Technology North Bangkok, Bangsue, Bangkok, 10800, THAILAND (e-mail: drpoolsak@gmail.com).

J. Koseeyaporn and P. Wardkein are with Faculty of Engineering, Department of Telecommunications Engineering, King Mongkut's Institute of Technology Ladkrabang, Ladkrabang, Bangkok, 10520, THAILAND (e-mail: jeerasuda@telecom.kmitl.ac.th, pramote@telecom.kmitl.ac.th).

II. Relaxation Oscillator

In general, a structure of a relaxation oscillator [8, 9] is composed of 3 parts as shown in Fig. 1 (where a current source $i_{in}(t)$ is neglected). The first part is a capacitor (C) where the second part is a charge-pump circuit which supplies constant currents ($\pm I_{CP}$). The third part is a Schmitt trigger circuit where $V_{th,L}$ and $V_{th,H}$ are two threshold voltages. The natural period of the oscillating signal, consisting of charge time (τ_H) and discharge time (τ_L), is $T_{nat} = 2C\Delta V_{th} / I_{CP}$ where $\Delta V_{th} = V_{th,H} - V_{th,L}$.

III. Relaxation Oscillator Injected by an Input Signal

In this article, studying behaviors of ILRO is considered in case of an input signal is sinusoidal signal. Let the input function be $i_{in}(t) = I_{in}\sin(\omega_{in}t)$ where I_{in} and ω_{in} are amplitude and frequency, respectively.

Physical behavior and locking condition of ILRO

The signal-generating process of the relaxation oscillator comprises of charging and discharging of the capacitor. For generating the suitable output signal, it is necessary that the charge time (τ_H) must be equal to the discharge time (τ_L).

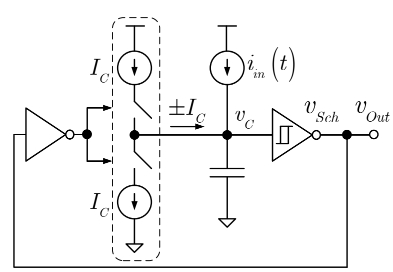

Fig. 1. A structure of the relaxation oscillator which is fed by an input signal

ISBN: 978-988-19253-9-8
ISSN: 2078-0958 (Print); ISSN: 2078-0966 (Online)

In other words, the current magnitude ($+I_{CP}$) of the charge pump circuit which is delivered to the capacitor is equal to the current magnitude ($-I_{CP}$) of the charge pump circuit which is derived from the capacitor. Therefore, to adjust the output period to correspond to the input period, average amplitude of the input amplitude in the charge time has to be equal to average amplitude of the input signal in the discharge time but opposite sign. With this physical behavior of the ILRO, the shape and, especially, the period of the input signal have an influence on the ILRO. However, the influence of the shape is less than that of the period, therefore, only the influence of the input period is considered to determine the locking condition.

When the oscillator locks to the input signal where $T_{in} = T/n$, n is the integer number and T is the detuned period of the output signal. The equation employed to determine the charge time of ILRO can be written as

$$\int_{v_C(t_1)}^{v_C(t_{1+1/2})} dv_C(t) = \frac{1}{C}\int_{t_1}^{t_{1+1/2}} \left[I_{CP} + I_{in}\sin\left(\omega_{in}\left(t+t_d\right)\right)\right]dt \qquad (1)$$

where t_d is the delay time. Define $t_1 = 0$, $t_{1+1/2} = \tau_{1,H} = T/2$, $v_C(t_1) = V_{th,L}$ and $v_C(t_{1+1/2}) = V_{th,H}$. After solving (1), it yields

$$\Delta V_{th} = \left(I_{CP}T/2C\right) + \left(I_{in}T/n2\pi C\right)\cos\left(\omega_{in}t_d\right)\left[1-\cos\left(\pi n\right)\right]. \quad (2)$$

It is found that voltage of the capacitor changed from $V_{th,L}$ to $V_{th,H}$ consists of two parts. The first part is $I_{CP}T/2C$ due to the charge-pump circuit. The other part is $\left[I_{in}T/2Cn\pi\right]\left[1-\cos\left(\pi n\right)\right]\cos\left(\omega_{in}t_d\right)$ which stems from the input signal. In case the input period is T/n_{Odd} where $n_{Odd} = 1, 3, \ldots$ The voltage changing of the capacitor from $V_{th,L}$ to $V_{th,H}$ is

$$\Delta V_{th} = \left(I_{CP}T/2C\right) + \left(I_{in}T/n_{Odd}\pi C\right)\cos\left(\omega_{in}t_d\right) \qquad (3)$$

From the relationship that $T_{nat} = 2C\Delta V_{th}/I_{CP}$ and $-1 \le \cos\left(\omega t_d\right) \le 1$, (3) will become

$$T_{nat}/\left(1+2\alpha/n_{Odd}\pi\right) \le T \le T_{nat}/\left(1-2\alpha/n_{Odd}\pi\right) \qquad (4)$$

where $\alpha = I_{in}/I_{CP}$. This equation points out that the output period can be detuned from the natural period (T_{nat}) to $T_{nat}/\left(1\pm\left(2\alpha/n_{Odd}\pi\right)\right)$. In case the input period is T/n_{Even} where $n_{Even} = 2, 4, 6, \ldots$, the voltage changing of the capacitor from $V_{th,L}$ to $V_{th,H}$ is

$$\Delta V_{th} = I_{CP}T/2C \qquad (5)$$

From (5), it is found that the voltage due to the input signal is absent. After rearranging this equation, it can be rewritten as

$$T_{nat} = T = n_{Even}T_{in} \qquad (6)$$

This equation points out that the oscillator will lock the input signal when the input period is $1/n_{Even}$ times of the natural period and the output period cannot be detuned like the n_{Odd} case. From Fig. 2, (6) is used to be boundaries of odd-harmonic locked ranges, and (4) is odd-harmonic locked ranges whose width is directly proportion to α.

IV. Behaviors of ILRO when the Input Frequency is in the $n_{Odd}f_{nat}$ Range

A. *The relationship between the input signal and the output signal*

Because of the signal-generating process of relaxation oscillator and the input signal being a function of time, behaviors of the ILRO will be considered cycle-by-cycle. In other words, the variation of the charge and discharge times due to the input signal will be considered from the cycle-m^{th} variation to the cycle-$(m+1)^{th}$ variation as shown in Fig. 3. When the input frequency is in the $n_{Odd}f_{nat}$ range, the oscillator will try to adjust the output period (T_m) of each cycle to $n_{Odd}T_{in}$. With this adjusting process, a relationship between the input signal and output signal is determined by using delay times, $t_{d,m}$ and $t_{d,m+1/2}$.

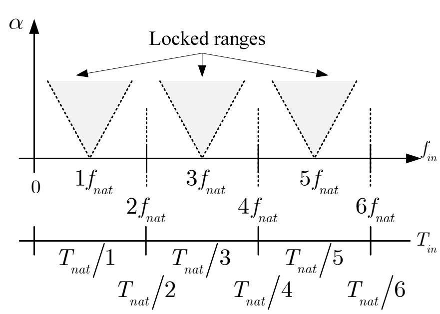

Fig. 2. Boundaries and locked ranges of each harmonic of the ILRO

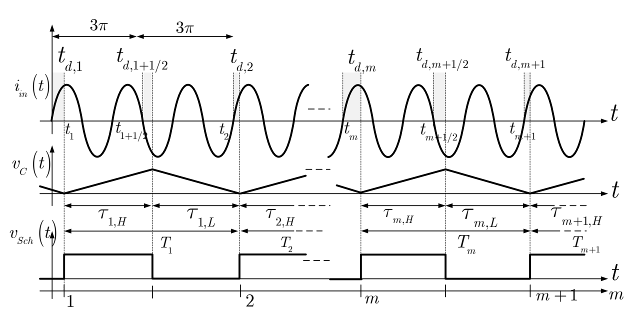

Fig. 3. The relationship between the input signal and the output signal when the input frequency is in the $3f_{in}$ range

ISBN: 978-988-19253-9-8
ISSN: 2078-0958 (Print); ISSN: 2078-0966 (Online)

The delay time, $t_{d,m}$, is an amount of time between the input-signal zero-crossing time at $\omega_{in}\left(t_m - t_{d,m}\right) = 0 \ or \ 2\pi$ and the time where the capacitor starts to charge (t_m) as shown in Fig. 3. Similarly, $t_{d,m+1/2}$ is the delay time which is an amount of time between the input-signal zero-crossing time at $\omega_{in}\left(t_{m+1/2} + t_{d,m+1/2}\right) = \pi$ and the time where the capacitor starts discharging ($t_{m+1/2}$). Moreover, from Fig. 3, the relationship between $t_{d,m}$ and $t_{d,m+1}$ is

$$t_{d,m+1} = \left(T_m + t_{d,m}\right) - n\left(2\pi / \omega_{in}\right) \tag{7}$$

This equation points out that the delay time depends on the period (T_m), hence, the procedure for determining T_m will be followed. The equation used for determining the charge time can be written as

$$\int_{v_C(t_m)}^{v_C(t_{m+1/2})} dv_C(t) = \frac{1}{C}\int_{t_m}^{t_{m+1/2}} \left[I_{CP} + I_{in}\sin\left(\omega_{in}\left(t + t_{d,m}\right)\right)\right]dt \tag{8}$$

where $v_C\left(t_m\right) = V_{th,L}$ and $v_C\left(t_{m+1/2}\right) = V_{th,H}$. After solving this integral equation, the charge time equation is

$$\tau_{m,H} = \frac{T_{nat}}{2} + \frac{\alpha}{\omega_{in}}\left[\cos\left(\omega_{in}\left(\tau_{m,H} + t_{d,m}\right)\right) - \cos\left(\omega_{in} t_{d,m}\right)\right] \tag{9}$$

where $\alpha = I_{in}/I_{CP}$, $t_m = 0$ and $t_{m+1/2} = \tau_{m,H}$. The integral equation used to determine the discharge time is

$$\int_{v_C(t_{m+1/2})}^{v_C(t_{m+1})} dv_C(t) = \frac{1}{C}\int_{t_{m+1/2}}^{t_{m+1}} \left[-I_{CP} + I_{in}\sin\left(\omega_{in}\left(t + t_{d,m}\right)\right)\right]dt \tag{10}$$

where $v_C\left(t_{m+1}\right) = V_{th,L}$. After solving (10), the discharge time is

$$\tau_{m,L} = \frac{T_{nat}}{2} - \frac{\alpha}{\omega_{in}}\left[\begin{array}{l}\cos\left(\omega_{in}\left(\tau_{m,H} + \tau_{m,L} + t_{d,m}\right)\right)\\ -\cos\left(\omega_{in}\left(\tau_{m,H} + t_{d,m}\right)\right)\end{array}\right] \tag{11}$$

where $t_{m+1} = \tau_{m,H} + \tau_{m,L}$. From (9) and (11), the period at the cycle-m^{th} is

$$\begin{aligned}T_m &= T_{nat} + \left(2\alpha / \omega_{in}\right)\cos\left(\omega_{in}\left(\tau_{m,H} + t_{d,m}\right)\right)\\ &-\left(2\alpha/\omega_{in}\right)\cos\left(\omega_{in}T_m/2 + \omega_{in}t_{d,m}\right)\cos\left(\omega_{in}T_m/2\right)\end{aligned} \tag{12}$$

Substituting (9) and (11) for $\tau_{m,H}$ and $\tau_{m,L}$, respectively, then using Taylor's series and neglecting the higher order terms of α, the output period is

$$T_m = T_{nat} + \left(k_2/\omega_{in}\right)\cos\left(k_0/2 + \omega_{in}t_{d,m}\right) \tag{13}$$

Where $k_0 = \left(\omega_{in} - n_{Odd}\,\omega_{nat}\right)T_{nat} + n_{Odd}\,2\pi$, $k_1 = \Delta\omega T_{nat}$, $k_2 = 4\alpha\cos^2\left(\Delta\omega T_{nat}/4\right)$ and $\Delta\omega = \omega_{in} - n_{Odd}\,\omega_{nat}$. Note that (13) is valid, if I_{in} is much less than I_{CP}. By substituting (13) into (7), it thus yields

$$\Delta t_{d,m} = \left(k_1 / \omega_{in}\right) + \left(k_2/\omega_{in}\right)\cos\left(k_0/2 + \omega_{in}t_{d,m}\right) \tag{14}$$

To gain insight into the behaviors of ILRO, $t_{d,m}$ will be considered as the continuous variable and (14) can be rewritten as

$$dt_d\left(m\right)/dm = \left(k_1/\omega_{in}\right) + \left(k_2 / \omega_{in}\right)\cos\left(k_0 / 2 + \omega_{in}t_d\left(m\right)\right) \tag{15}$$

and

$$\int_0^{t_d(m)} \frac{dt_d\left(m\right)}{1 + K\cos\left(k_0/2 + \omega_{in}t_{d,m}\right)} = \frac{k_1}{\omega_{in}}\int_0^m dm \tag{16}$$

where $K = k_2/k_1$. By solving this integral equation, the continuous delay time thus is

$$\begin{aligned}t_d\left(m\right) &= -\left(k_0/2\omega_{in}\right)\\ &+\frac{2}{\omega_{in}}\tan^{-1}\left(\frac{1+K}{\sqrt{1-K^2}}\tan\left(\frac{k_1\sqrt{1-K^2}}{2}m + C_t\right)\right)\end{aligned} \tag{17}$$

where $C_t = \tan^{-1}\left(\frac{\sqrt{1-K^2}}{1+K}\tan\left(\frac{k_0}{4} + \frac{\omega_{in}t_d\left(0\right)}{2}\right)\right)$. From (17), $t_d\left(m\right)$ has the periodic variation which depends on K. Because $\left|K\right|$ is dependent on amplitude and frequency of the input signal, the variations of $\left|K\right|$ which are due to these factors can be shown in Fig. 4. It is noted that the discontinuous position of graph means that the values converge to infinity. It is seen that the more the input frequency moves close to $3f_{nat}$, the more $\left|K\right|$ get increases. Moreover, increasing of the input amplitude will accelerate an increasing of $\left|K\right|$. When considering both $\left|K\right|$ and $\sqrt{1-K^2}$, $\left|K\right|$ can be divided into two parts, $\left|K\right| < 1$ and $\left|K\right| \geq 1$ which will be discussed in the next subsection.

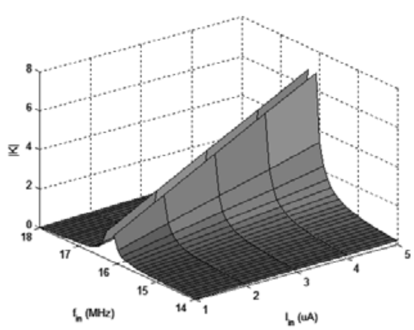

Fig. 4. A variation of $\left|K\right|$ due to amplitude and frequency of the input signal whose f_{nat} and I_{CP} of the relaxation oscillator are 5.42MHz and 25uA, respectively and the input frequency is in the $3f_{nat}$ range.

ISBN: 978-988-19253-9-8
ISSN: 2078-0958 (Print); ISSN: 2078-0966 (Online)

B. The output period detuning process ($|K|<1$)

For considering $t_d(m)$ in practical, it may be impossible because this parameter is small and varies all the time. Therefore, the output period will be used to study the oscillator behaviors instead of $t_d(m)$. By substituting $t_d(m)$ of (17) into $T(m)$ which is considered to be the continuous variable, the output period can be rewritten as

$$T(m)=T_{nat}-(k_1/\omega_{in})\left(1-\sqrt{1-K^2}\right)+\frac{2k_1}{\omega_{in}}\sqrt{1-K^2}\sum_{p=1}^{\infty}r^p\cos\left(p\left(k_1\sqrt{1-K^2}m+2C_t\right)\right) \quad (18)$$

where $r=\left(1-\sqrt{1-K^2}\right)\big/K$. This equation shows that the output period composes of two terms. The first term is a constant value. The second term is a periodic function of m whose period is

$$M=2\pi\Big/\left(k_1\sqrt{1-K^2}\right) \quad (19)$$

The second term reaches its maximum and minimum values if $2\pi m/M+2C_t=0,2\pi,4\pi,...$ and $2\pi m/M+2C_t=\pi,3\pi,5\pi,...,$ respectively. The pattern of variation of this term is very interesting when the value of M changes. For small M, $T(m)$ will quickly change from the maximum value to the minimum value. It is also found that if the input frequency (f_{in}) moves close to $n_{Odd}f_{nat}$, M will increase and the rate of the variation of $T(m)$ will decrease. The slower variation of $T(m)$ implies that the output period is adjusting to the period of the input signal. This behavior of deviation of the output period is demonstrated in Fig. 5. Moreover, the relationship between the m-domain and the time-domain of the output signal is also illustrated. For convenience of considering the influence of amplitude and frequency of the input signal, average of the output period is also employed to study the oscillator behavior active in a pulling state.

$$\overline{T(m)}=T_{nat}-(k_1/\omega_{in})\left(1-\sqrt{1-K^2}\right) \quad (20)$$

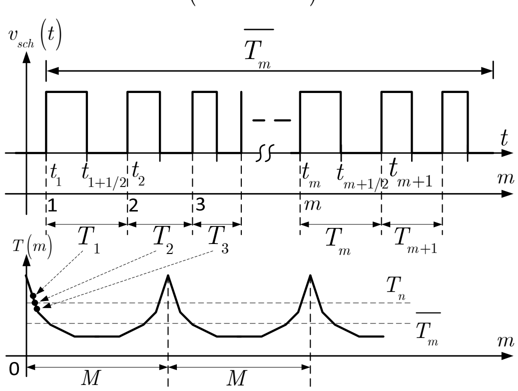

Fig 5. The relationship between the time-domain output signal and the m-domain output period.

From (20) and $K=k_2/k_1$, it is found that when the input frequency moves close to the locked range, $\overline{T(m)}$ will also move close to the period of the input period.

C. Locking State ($|K|\geq 1$)

For $|K|\geq 1$, (17) becomes

$$t_d(m)=-k_0/2\omega_{in}+\frac{2}{\omega_{in}}\tan^{-1}\left(\frac{j(K+1)}{\sqrt{K^2-1}}\tan\left(\begin{array}{l}\left((jk_1m/2)\sqrt{K^2-1}\right)\\+jC_{t,locked}\end{array}\right)\right) \quad (21)$$

where $C_{t,locked}$ is a constant value which is derived from solving the integral equation. By using the trigonometric identity $\tanh(\theta)=-j\tan(j\theta)$, (21) will be

$$t_d(m)=-\frac{k_0}{2\omega_{in}}-\frac{2}{\omega_{in}}\tan^{-1}\left(\frac{K+1}{\sqrt{K^2-1}}\right) \quad (22)$$

By substituting $t_d(m)$ of (22) into $T(m)$ and using a trigonometric identity, the output period can be rewritten as

$$T(m)=n_{Odd}T_{in}. \quad (23)$$

From (23), it is found that for $|K|\geq 1$, the oscillator behavior will move to the locked state and the output period will be n_{Odd} times of the input period. Based on this behavior of the ILRO, the locked range determined by using the relationship of $|K|\geq 1$ can be written as $\left|4\alpha\cos^2(\Delta\omega T_{nat}/4)/\Delta\omega T_{nat}\right|\geq 1$. When the oscillator is in the locked state, $\cos^2(\Delta\omega T_{nat}/4)\approx 1$. Hence,

$$|\Delta\omega|\leq\left(4I_{in}/T_{nat}I_{CP}\right) \quad (24)$$

From this equation, the input-frequency range which the oscillator will lock, therefore is

$$\left(n_{Odd}\omega_{nat}-|\Delta\omega|\right)\leq\omega_i\leq\left(n_{Odd}\omega_{nat}+|\Delta\omega|\right) \quad (25)$$

Because $|\Delta\omega|=|\omega_{in}-n_{Odd}\omega_{nat}|$, the locked range of each $n_{Odd}f_{nat}$ range is equal. Moreover, (25) is similar to (4) which determines the locking condition. With this behavior of the oscillator and equal locked range for all $n_{Odd}f_{nat}$, the relaxation oscillator is therefore easy to be applied for the synchronization oscillator in case $n_{Odd}=1$ and the frequency divider in case $n_{Odd}=3,5,...$.

V. SIMULATION AND CALCULATION RESULTS

In this paper, the basic relaxation oscillator is used to study the behaviors of the ILRO as shown in Fig. 6. This oscillator is designed by 0.35um-CMOS technology of TSMC and the dimension of each MOS is showed in Table

ISBN: 978-988-19253-9-8
ISSN: 2078-0958 (Print); ISSN: 2078-0966 (Online)

1. The Schmitt trigger circuit has 2 threshold voltages, which are 0.65V and 2.75V. The charge-pump circuit is designed to deliver 25uA. The capacitor has a capacitance of 1pF. The supply voltage is 3.3V. The simulation output of the oscillator without the input signal is shown in Fig. 7. These signals illustrate that the charge time and the discharge time are equal because there is no any disturbance. The output period is 0.1845uS or the output frequency is 5.42MHz.

A. The output period of each cycle (T_m)

Fig. 8 is an example of the oscillator behavior when the input frequency is in the $3f_{nat}$ range. It is found that the output signal deviates from the natural period (0.1845uS) and this deviation moves close to $3T_{in}$. The more the input frequency moves close to the locked range, the more the output period moves close to $3T_{in}$. Not only the output period moves close to $3T_{in}$ but also the variation from the maximum value to the minimum value gets slower than and the M period gets wider. Moreover, the calculation results of (18) are also similar to the simulation results.

B. Average output period ($\overline{T(m)}$)

Fig. 9 shows comparison between the simulation results and the calculation result from (20) of the average output periods of $1f_{nat}$, $3f_{nat}$ and $5f_{nat}$ ranges. It is found that the output period will deviate from the natural period, 0.1845uS, and moves close to $n_{Odd}T_{in}$. Moreover, when the input frequency moves to the locked range, the output period will equal to $n_{Odd}T_{in}$.

C. The periodic variation (M) of the cycle-m^{th} of the output period

From the simulation results in Fig.8, it is seen that when the input frequency moves close to the locked range, the variation of the output period will be slower, in other words, the period of M gets increase. This behavior appears in every $n_{Odd}f_{nat}$ range as the simulation results depicted in Fig.10. Moreover, the cycle variation of the simulation results and the calculation results are similar.

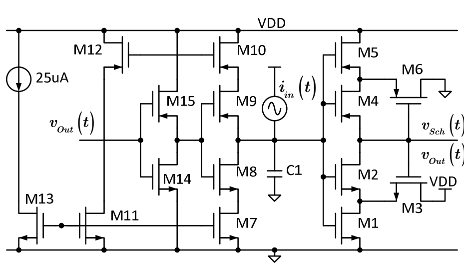

Fig. 6. The structure of relaxation oscillator.

TABLE 1.
DIMENSION OF TRANSISTORS

Device names	W(um)/L(um)
M1, 2, 7, 8, 11, 13, 14	4.2/0.7
M3	25/0.7
M4, 5, 9, 10, 12, 15	14/0.7
M6	70/0.7

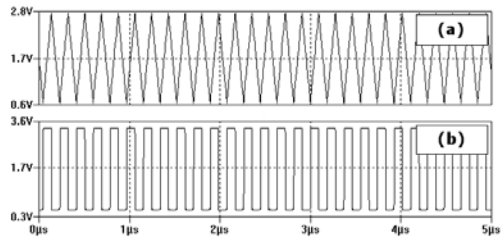

Fig. 7. The simulation outputs of the relaxation oscillator without the input signal where (a) is $v_C(t)$ and (b) is $v_{Sch}(t)$.

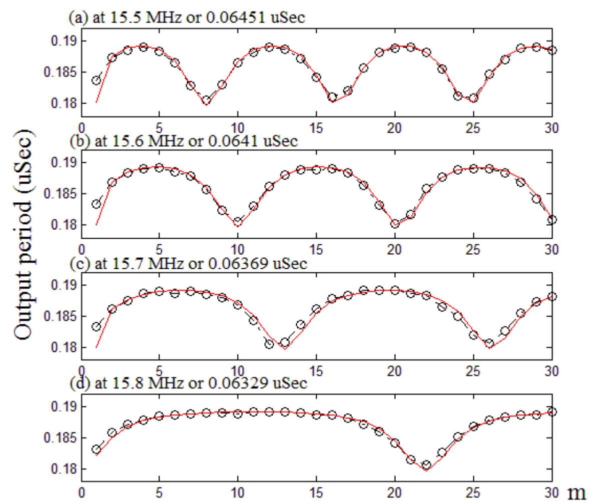

Fig. 8. The variation of each cycle when the input signal has amplitude of 3uA and frequency is in the $3f_{nat}$ range where (-o-) is simulation results and (--) is calculation results.

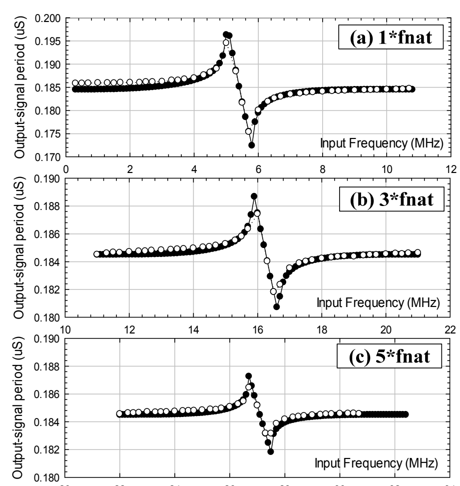

Fig, 9. The simulation result and the calculation result of the average output-signal period when the input amplitude is 3uA.

D. Locking behavior of the oscillator($|K| \geq 1$)

When the input frequency is in the $1f_{nat}$ range, the oscillator shows the synchronizing behavior that is the oscillator generates the output signal whose rhythm is similar to the input signal (see Fig.11). When the input signal is in the $3f_{nat}$ range, the results are given in Fig 12. Not only the output signal synchronizes the input signal, but also the output signal is a dividing result of the input signal at ratio 1/3. Fig. 13 is the simulation result when the

ISBN: 978-988-19253-9-8
ISSN: 2078-0958 (Print); ISSN: 2078-0966 (Online)

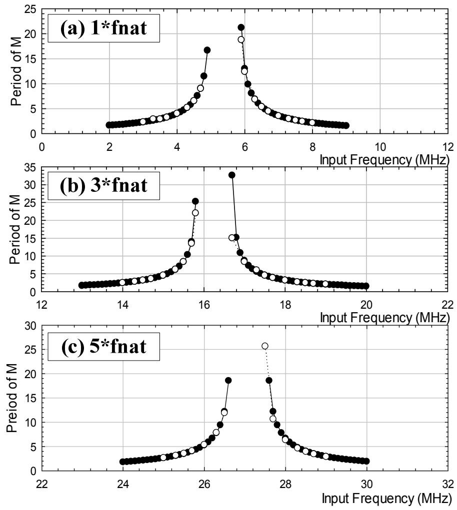

Fig.10. The simulation results and the calculation results of the M period when the input signal has amplitude of 3uA where (○) is simulation results and (●) is calculation results

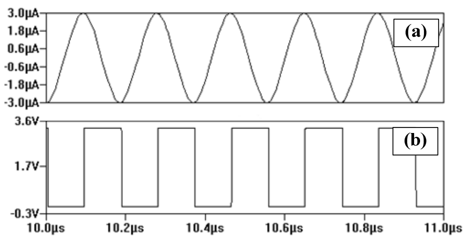

Fig. 11. The simulation result when the oscillator is in locked state and in the $1f_{nat}$ range where (a) is the input signal whose amplitude is 3uA and frequency is 5.4MHz and (b) is the output signal.

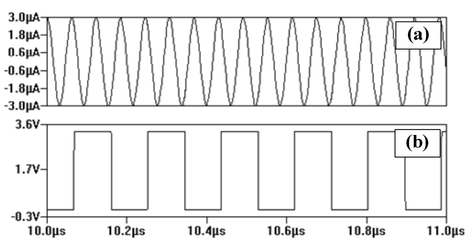

Fig. 12. The simulation result when the oscillator is in locked state and in the $3f_{nat}$ range where (a) is the input signal whose amplitude is 3uA and frequency is 16.2MHz and (b) is the output signal.

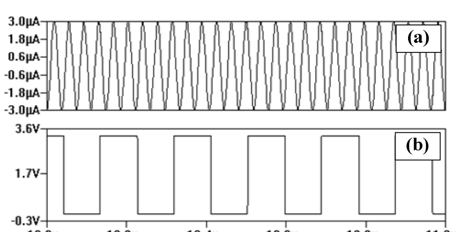

Fig. 13. The simulation result when the oscillator is in locked state and in the $5f_{nat}$ range where (a) is the input signal whose amplitude is 3uA and frequency is 27MHz and (b) is the output signal.

input signal is in the $5f_{nat}$ range. The oscillator shows behavior similar to that of the $3f_{nat}$ case but the dividing ratio is 1/5. Fig. 14 is the locked-range comparison between the simulation result and the calculation result of each range ($1f_{nat}$, $3f_{nat}$ and $5f_{nat}$). From this figure, the V-shape characteristic of the locked range implies that the locked

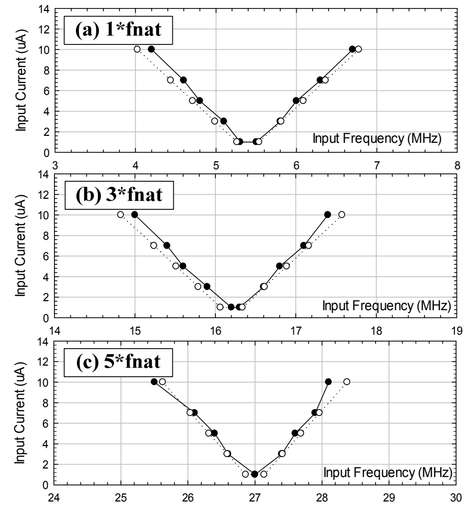

Fig. 14. The simulation results and calculation results of the locked ranges of the ILRO where (●) is simulation results and (○) is calculation results

range directly depends on the input amplitude. Moreover, the locked range of each frequency range is equal.

VI. CONCLUSIONS

In this article, the enhanced mathematical model is proposed to study behaviors of the ILRO. The proposed technique considers the time variations of the output signal cycle-by-cycle due to the input signal which occurs during in the charge time and the discharge time. Moreover, the simulation results show that the proposed model can be clearly explained behaviors of the ILRO.

REFERENCES

[1] R. Adler, “A study of locking phenomena in oscillators,” *Proceedings of the IEEE*, 1973, vol. 61, no. 10, p. 1380 – 1386.

[2] B. Razavi, “A study of injection locking and pulling in oscillators,” *IEEE Journal of Solid-State Circuits*, 2004, vol.39. no. 9, p. 1415 – 1425.

[3] B. N. Biswas, S. Chatterjee, S. Pai, “New observations on bias current variation of op amp oscillators,” In *Proceedings of General Assembly and Scientific Symposium*, 2011, p. 1- 4.

[4] P. Maffezzoni, D. D’Amore, “Evaluating pulling effects in oscillators,” *IEEE Transaction on Computer-Aided Design of Integrated Circuits and Systems,* 2009, vol. 28, no. 1, p. 22 - 31.

[5] P. Maffezzoni, “Analysis of oscillator injection locking through phase-domain impulse-response,” *IEEE Transactions on Circuits and Systems I: Fundamental Theory and Applications*, 2008, vol. 55, p. 1297-1305.

[6] P. Maffezzoi, D. D’Amore, S. Daneshgar, M. P. Kennedy, “Analysis and Design of Injection-Locked Frequency Dividers by Means of a Phase-Domain Macromedel,” *IEEE Transaction Circuits and Systems,* 2010, vol. 57, no. 11, p. 2956 - 2966.

[7] S. NIMA, Y. Fel, “Nonharmonic injection-locked phase-locked loops with applications in remote frequency calibration of passive wireless transponders,” *IEEE Transaction Circuits and Systems,* 2010, vol. 57, no. 9, p. 2381 - 2393.

[8] J. B. Russel, *CMOS Circuit Design, Layout, and Simulation, Second Edition*. Wiley-IEEE Press, 2005.

[9] G. Guillermo, *Foundations of Oscillator Circuit Design*, Artech house, 2007.

ISBN: 978-988-19253-9-8
ISSN: 2078-0958 (Print); ISSN: 2078-0966 (Online)